

Research Article

Depletion of high-mobility group box 2 causes seminiferous tubule atrophy via aberrant expression of androgen and estrogen receptors in mouse testis[†]

Naohiro Sugita^{1,2,‡}, Narantsog Choijookhuu^{1,‡}, Koichi Yano^{1,3},
Deokcheol Lee⁴, Makoto Ikenoue^{1,3}, Fidya¹, Noboru Taniguchi⁵,
Etsuo Chosa⁴ and Yoshitaka Hishikawa^{1,*}

¹Department of Anatomy, Histochemistry and Cell Biology, Faculty of Medicine, University of Miyazaki, Miyazaki, Japan, ²Department of Ophthalmology, Faculty of Medicine, University of Miyazaki, Miyazaki, Japan, ³Department of Surgery, Faculty of Medicine, University of Miyazaki, Miyazaki, Japan, ⁴Department of Orthopaedic Surgery, Faculty of Medicine, University of Miyazaki, Miyazaki, Japan and ⁵Department of Orthopaedic Surgery, Graduate School of Medical and Dental Sciences, Kagoshima University, Kagoshima, Japan

***Correspondence:** Department of Anatomy, Histochemistry and Cell Biology, Faculty of Medicine, University of Miyazaki, 5200 Kihara, Kiyotake, Miyazaki 889-1692, Japan. Tel: +81985851783; Fax: +81985859851; E-mail: yhishi@med.miyazaki-u.ac.jp

[†]**Grant Support:** This study was supported in part by a grant-in-aid for Scientific Research from the Japan Society for the Promotion of Science (Nos. 16K08471 and 21K06738 to YH and No. 19K16477 to NC).

[‡]These authors contributed equally to this study.

Received 10 June 2021; Revised 25 August 2021; Accepted 1 October 2021

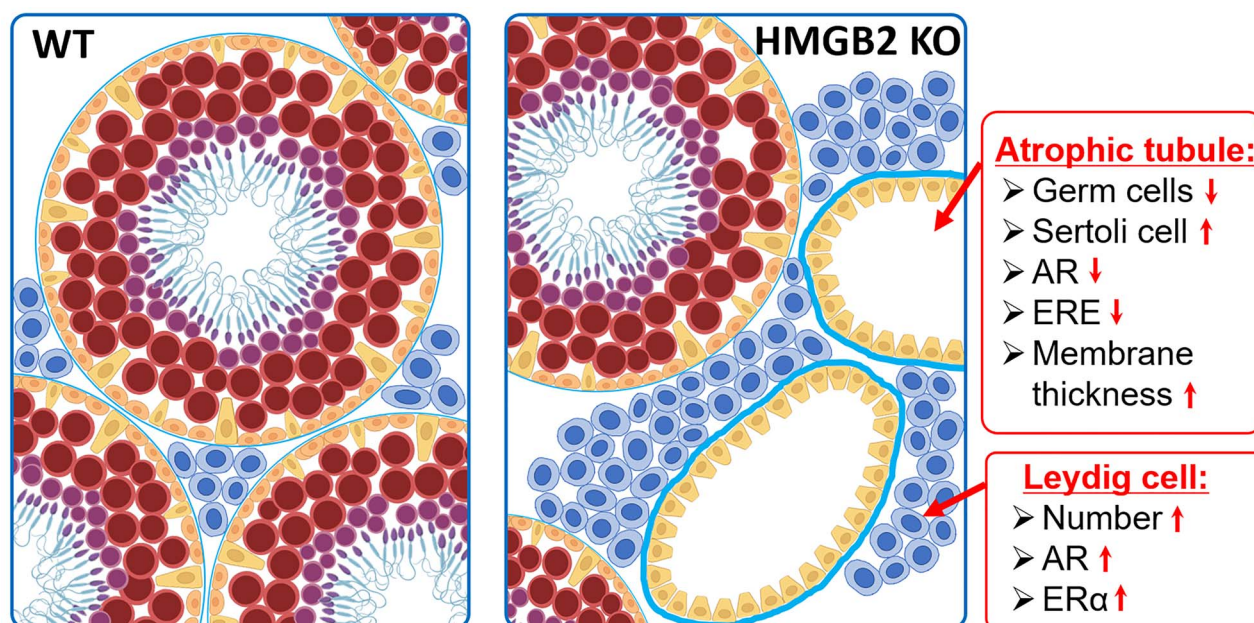
Abstract

High-mobility group box 2, a chromatin-associated protein that interacts with deoxyribonucleic acid, is implicated in multiple biological processes, including gene transcription, replication, and repair. High-mobility group box 2 is expressed in several tissues, including the testis; however, its functional role is largely unknown. Here, we elucidated the role of high-mobility group box 2 in spermatogenesis. Paraffin-embedded testicular tissues were obtained from 8-week-old and 1-year-old wild-type and knock-out mice. Testis weight and number of seminiferous tubules were decreased, whereas atrophic tubules were increased in high-mobility group box 2-depleted mice. Immunohistochemistry revealed that atrophic tubules contained Sertoli cells, but not germ cells. Moreover, decreased cell proliferation and increased apoptosis were demonstrated in high-mobility group box 2-depleted mouse testis. To elucidate the cause of tubule atrophy, we examined the expression of androgen and estrogen receptors, and the results indicated aberrant expression of androgen receptor and estrogen receptor alpha in Sertoli and Leydig cells. Southwestern histochemistry detected decreased estrogen response element-binding sites in high-mobility group box 2-depleted mouse testis. High-mobility group box 1, which has highly similar structure and function as high-mobility group box 2, was examined by immunohistochemistry and western blotting, which indicated increased expression in testis. These findings indicate a compensatory increase in high-mobility group box 1 expression in high-mobility group box 2 knock-out mouse testis. In summary, depletion of high-mobility group box 2 induced aberrant expression of androgen receptor and estrogen receptor alpha, leading to decreased germ cell proliferation and increased apoptosis which resulted in focal seminiferous tubule atrophy.

Summary sentence

Depletion of High-mobility group box 2 induced aberrant androgen receptor and estrogen receptor alpha expression, leading to decreased germ cell proliferation and increased apoptosis, resulting in seminiferous tubule atrophy.

Graphical Abstract



Key words: HMGB2, testis, androgen receptor, estrogen receptor, tubule atrophy.

Introduction

High-mobility group (HMG) proteins are the most abundant non-histone chromatin-associated proteins involved in gene transcription, replication, recombination, and repair processes [1]. High-mobility group box 2 (HMGB2) is a member of the HMG protein family characterized by two unique HMG box DNA-binding domains that are involved in DNA distortion by bending, unwinding, or looping to facilitate the assembly of multiprotein complexes on DNA [2]. Similar to other HMG group proteins, HMGB2 is involved in fine-tuning of gene transcription [3]. The HMGB2 is depleted in senescent cells and aging tissues but is dramatically increased in various cancers [4–6]. A number of studies revealed that HMGB2 is associated with cell proliferation and the transition of cells from the quiescent to active state [7, 8]. The testis, which is a highly proliferative tissue, is affected by HMGB2 depletion [9]. Although HMGB2-depleted mice exhibit reduced fertility and defective spermatogenesis, the role of HMGB2 in spermatogenesis is largely unknown.

Spermatogenesis is an extraordinarily complex process regulated by multiple factors, including genetic, hormonal, environmental, and epigenetic regulators [10]. Among these factors, the sex steroid hormones are known to play critical roles in spermatogenesis via the androgen receptor (AR) and estrogen receptors (ERs) [11, 12]. Both the ARs and ERs are known to functionally interact with HMGB2 to enhance DNA-binding and transcriptional activity [13, 14]. Although these interactions have been examined in cell lines, the role of HMGB2 in spermatogenesis is not fully understood.

Structural and functional analyses revealed that HMGB2 is very similar to HMGB1, such as >80% of the amino acids are identical [15]. Despite the similarity between HMGB2 and HMGB1, their expression patterns differ throughout the body. Both proteins are abundantly expressed during embryonic development. However, in adults, HMGB1 is expressed ubiquitously throughout the body, whereas HMGB2 expression is restricted to the testis and lymphoid tissues [9]. Therefore, the functional relationship between HMGB1 and HMGB2 is still controversial.

In the present study, we first investigated the long-term role of HMGB2 in spermatogenesis using HMGB2 knock-out (KO) mice. Depletion of HMGB2 led to seminiferous tubule atrophy, possibly due to disruption of signaling by sex steroid hormones, such as androgens and estrogens, via their receptors. We found decreased germ cell proliferation and increased apoptosis in HMGB2 KO mouse testis. Expression of HMGB1 was observed in spermatocytes of HMGB2 KO mouse testis but not in wild-type (WT) littermates, suggesting that expression of HMGB1 was increased in a compensatory manner in HMGB2 KO mouse testis.

Materials and methods

Chemicals and biochemicals

Paraformaldehyde (PFA) was purchased from Merck (Darmstadt, Germany). Trizma base, bovine serum albumin (BSA), 2-mercaptoethanol, 3-aminopropyl-triethoxysilane, Triton X-100,

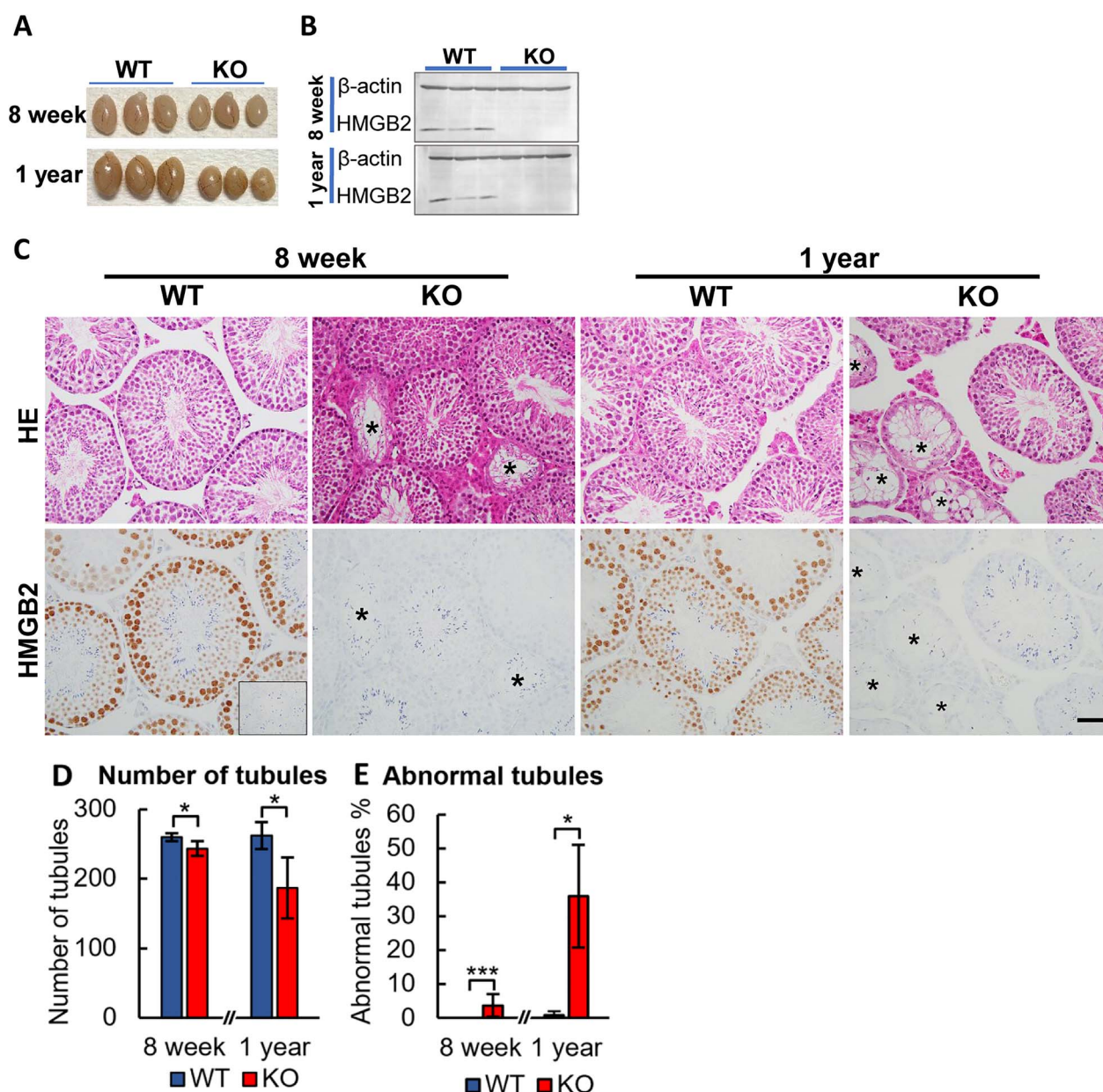


Figure 1. Seminiferous tubule atrophy in HMGB2 KO mouse testis. Macrophotography of WT and HMGB2 KO mouse testis at 8 weeks and 1 years of age (A). Western blotting analysis of HMGB2 in WT and KO mouse testis (B). HE staining and immunohistochemistry for HMGB2 were performed in serial sections of WT and HMGB2 KO mouse testis (C). Total (D) and abnormal seminiferous tubules (E) were counted in testicular cross-sections. Negative control is shown in the inset. Asterisks indicate atrophic tubules. Scale bar: 50 μ m. Graphs represents mean \pm SEM. In each experimental group, three to five mice were used. * P < 0.05, *** P < 0.001. Student's t -test (two-tailed).

Tyramine hydrochloride, and Brij L23 were purchased from Sigma Chemical Co. (St Louis, MO, USA). FITC- or rhodamine-succinimidyl esters and the BCA protein assay kit were purchased from Thermo Fisher (USA). Polyvinylidene fluoride (PVDF) membranes were purchased from Millipore (Bedford, MA, USA). Molecular marker sets were purchased from Biodynamics (Tokyo, Japan). The 3,3'-diaminobenzidine-4 HCl (DAB) was purchased from Dojindo Chemicals (Kumamoto, Japan). The Masson trichrome staining kit was obtained from Muto Pure Chemicals

(Tokyo, Japan). All other reagents used in this study were purchased from Fujifilm Wako Pure Chemicals (Osaka, Japan).

Animals and tissue preparation

Male C57BL/6 WT and HMGB2 KO mice (8 weeks and 1 years old) were used in the present study. The derivation of genomic HMGB2 KO mouse has been described [9]. Mice were fed with normal chow and were allowed to drink water ad libitum. The experimental protocol was approved by the Animal Ethics Review Committee

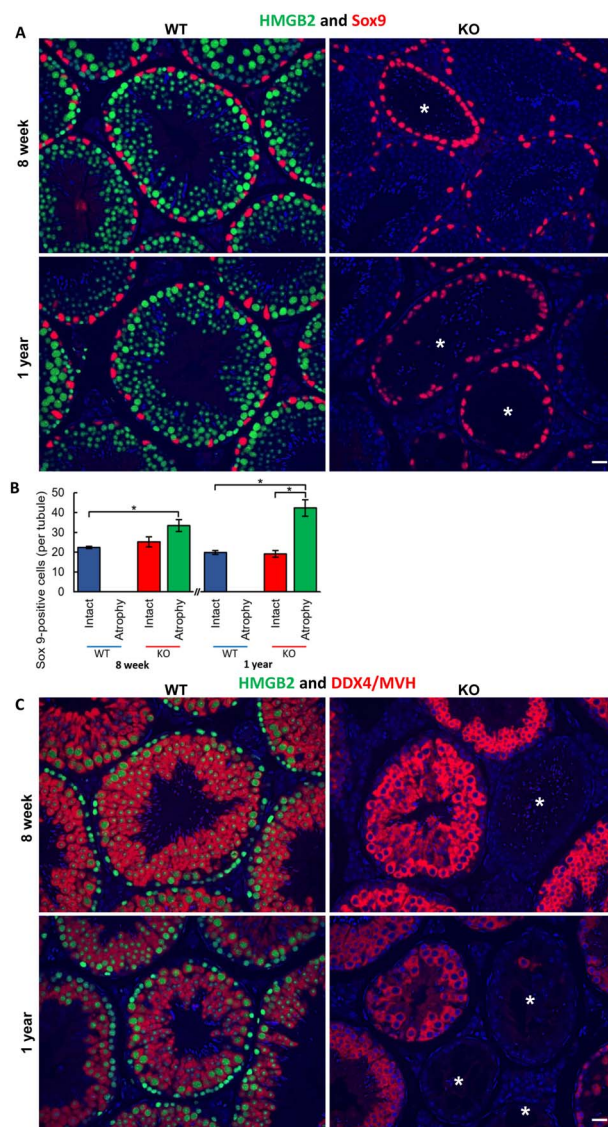


Figure 2. Expression of HMGB2 in the testis. Double immunofluorescence for HMGB2 (green) and Sox9 (red) in WT and HMGB2 KO mouse testis (A). Sox9-positive cells in intact and atrophic tubule in WT and HMGB2 KO mouse testis (B). Expression of HMGB2 (green) and DDX4/MVH (red) were also examined in paraffin-embedded tissue sections (C). Nuclear counterstaining was performed using DAPI (blue). Asterisks indicate atrophic tubules. Scale bar: 20 μ m. Graphs represents mean \pm SEM. In each experimental group, three to five mice were used. * $P < 0.05$. Student's t -test (two-tailed).

of the University of Miyazaki (2018-510-6). After animals were sacrificed, the left testis was snap frozen and kept at -80°C until used for western blotting. The right testis was fixed in 4% PFA in phosphate-buffered saline (PBS) (pH 7.4) for overnight at room temperature (RT) and was then embedded in paraffin. In each experimental group, three to five mice were used.

Histological analysis

Testicular morphology was analyzed by hematoxylin and eosin (HE) staining. Thickening of the tubule membrane was examined by Masson trichrome staining according to the manufacturer's instructions.

Immunohistochemistry

Paraffin-embedded tissues were cut into 4- μ m thick sections and were placed onto silane-coated slide glasses. The sections were deparaffinized with toluene and rehydrated using a graded ethanol series, then autoclaved at 120°C for 15 min in 10 mM citrate buffer (pH 6.0) [16, 17]. After inhibition of endogenous peroxidase activity with 3% H_2O_2 in methanol for 30 min, the sections were pre-incubated with 500 μ g/ml normal goat IgG and with 1% BSA in PBS for 1 h to block non-specific binding of antibodies. The sections were then reacted with the following primary antibodies for 16–17 h: anti-HMGB2 (Abcam, ab124670), anti-Sox9 (Atlas, HPA001758), anti-DDX4/MVH (Abcam, ab13840), anti-PCNA (Dako, M0879), anti-AR (Millipore, 06-680), anti-ER α (Thermo, MA5-13304), anti-HMGB1 (Abcam, ab18256), and anti-SCP3 (Abcam, ab97672). After washing with 0.075% Brij L23 in PBS, the sections were reacted with HRP-goat anti-mouse IgG or with HRP-goat anti-rabbit IgG for 1 h. After washing in 0.075% Brij L23 in PBS, the HRP sites were visualized with DAB and H_2O_2 . For immunofluorescence, sections were treated with FITC- or rhodamine-conjugated tyramide and were then counterstained with DAPI [18]. As a negative control, normal mouse or rabbit IgG was used at the same concentration instead of the primary antibody in each experiment. Microphotos were taken using a fluorescence microscope (Keyence BZ-X700) and light microscope (Olympus BX53).

Western blot analysis

Tissues were homogenized in hot SDS lysis buffer with a glass-teflon homogenizer, as described previously [19, 20]. After centrifugation of the homogenate at 15 000 rpm for 30 min at 4°C , the supernatant was collected and stored at -80°C . The protein concentration in each preparation was determined using a BCA assay kit. Lysate containing 20 μ g of protein was separated by 10% SDS-PAGE, and the proteins were electrophoretically transferred onto PVDF membranes. The membranes were blocked with 5% nonfat milk in Tris-buffered saline (TBS; 20 mM Tris buffer [pH 7.6], 150 mM NaCl) for 1 h at RT and were then incubated overnight with anti-HMGB2 or anti-HMGB1 antibodies diluted 1:1000 with TBS/0.05% Triton X-100 buffer. As a secondary antibody, HRP-goat anti-rabbit IgG or HRP-goat anti-mouse IgG was diluted with TBS buffer for 1 h, and the membranes were washed three times for 10 min each with TBS/0.05% Triton X-100 buffer. Bands were visualized with DAB, Ni, Co, and H_2O_2 . Densitometric analysis was performed using ImageQuant LAS 4000 (GE Healthcare, Fairfield, CT, USA). The β -actin was used as an internal standard in each lane for normalization of target protein expression.

TUNEL staining

The TUNEL staining was performed as described previously [21]. Briefly, the sections were deparaffinized with toluene and were rehydrated using a graded ethanol series. After washing with PBS, the sections were treated with 10 μ g/ml of proteinase K in PBS at 37°C for 15 min. The sections were then rinsed once with distilled water and incubated with TdT buffer (25 mM Tris-HCl buffer [pH 6.6], containing 0.2 M potassium cacodylate and 0.25 mg/ml BSA) alone for 30 min at RT. The sections were then reacted with 800 U/ml TdT dissolved in a TdT buffer supplemented with 5 μ M biotin-16-dUTP, 20 μ M dATP, 1.5 mM CoCl_2 , and 0.1 mM dithiothreitol at 37°C for 90 min. The reaction was terminated by washing with 50 mM Tris/HCl buffer (pH 7.5) for 15 min. Endogenous peroxidase activity was inhibited by immersing the slides in 0.3% H_2O_2 in methanol for

Table 1. BW and testis weight in WT and HMGB2 KO mouse

Age	BW (g)		Testis weight (mg)	
	WT	KO	WT	KO
8 weeks	22.3 ± 0.8	21.7 ± 0.6	90.7 ± 2.0	64.4 ± 2.1*
1 year	38.4 ± 2.6	34.0 ± 2.5	106 ± 3.6	61.4 ± 7.7**

Testis weight was compared with age-matched littermates.
**P* < 0.05.
***P* < 0.01.

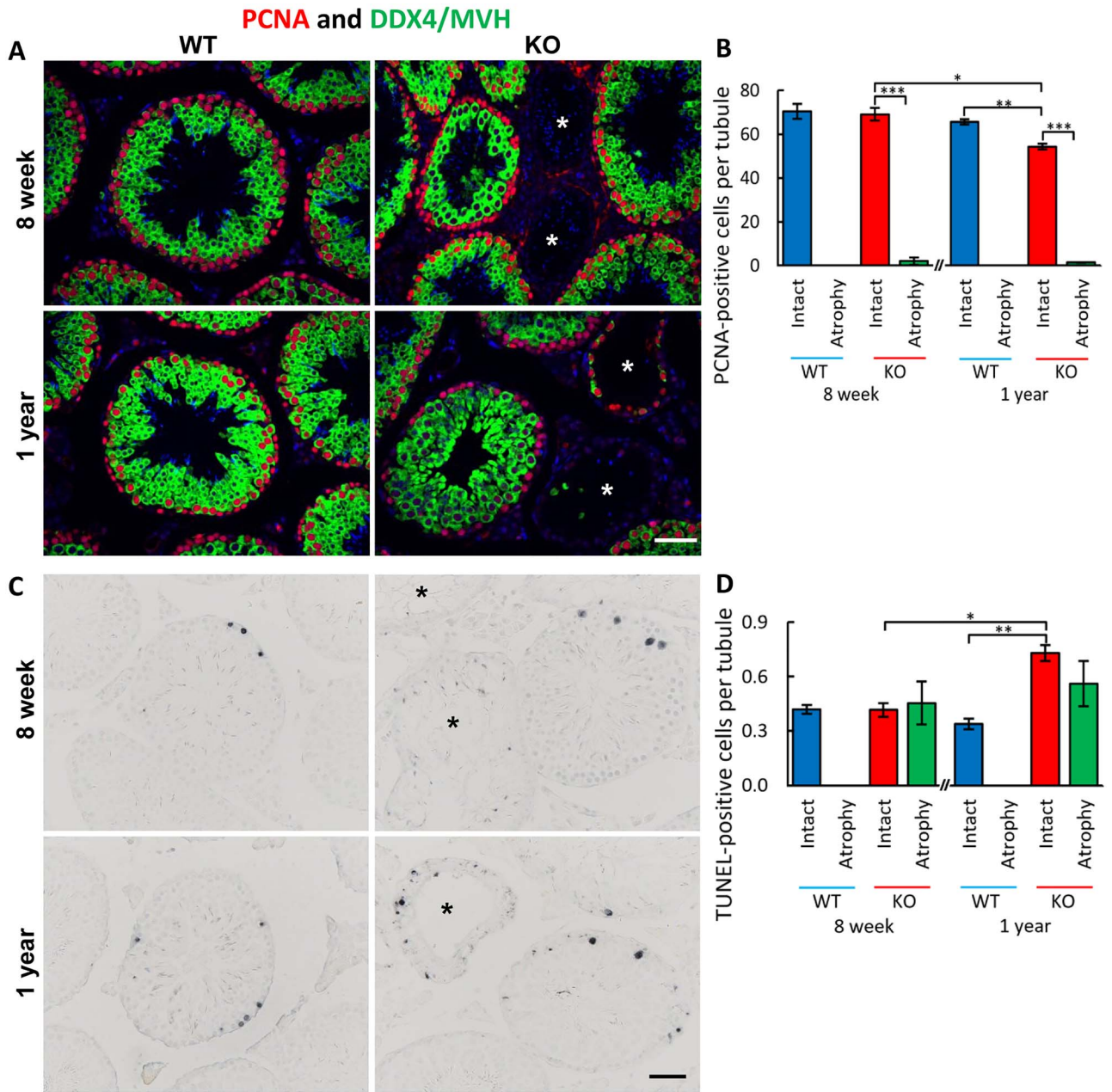


Figure 3. Cell proliferation and apoptosis in WT and HMGB2 KO mouse testis (A). Number of PCNA-positive cells in intact and atrophic tubules (B). Paraffin-embedded testicular sections were analyzed by TUNEL (C). Number of TUNEL-positive cells in intact and atrophic tubules (D). Asterisks indicate atrophic tubules. Graphs represent mean ± SEM. In each experimental group, three to five mice were used. Scale bar: 50 μm. **P* < 0.05, ***P* < 0.01, ****P* < 0.001. Student's *t*-test (two-tailed).

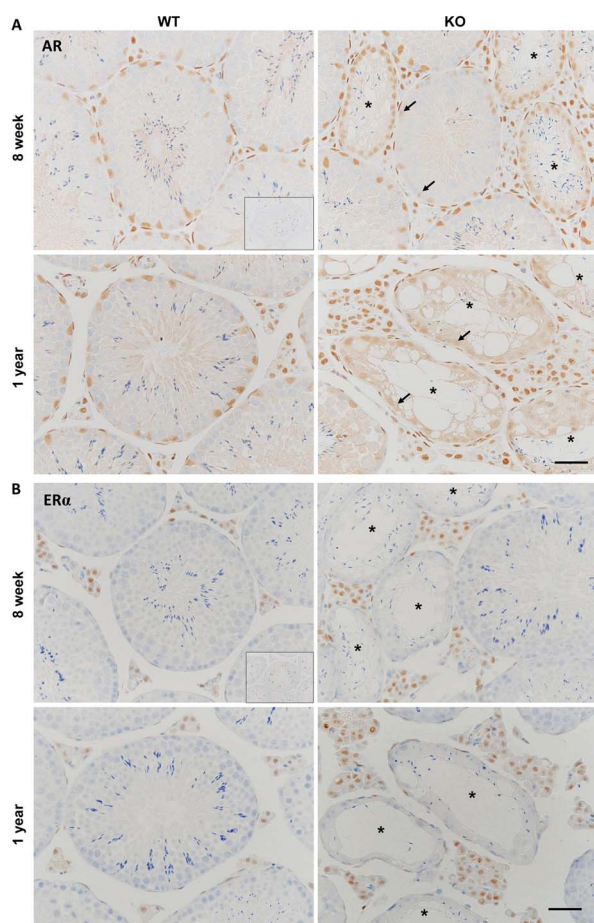


Figure 4. Aberrant expression of AR and ER α in HMGB2 KO mouse testis. Immunohistochemical localization of AR in WT and HMGB2 KO mouse testis (A). Arrows indicate decreased AR expression in Sertoli cells. Immunohistochemical localization of ER α in WT and HMGB2 KO mouse testis (B). Negative control is shown in the inset. Cell nuclei were counterstained with hematoxylin. Asterisks indicate atrophic tubules. Scale bar: 50 μ m.

15 min at RT. Signals were detected immunohistochemically using an HRP-conjugated goat anti-biotin antibody, and HRP sites were visualized by DAB, Ni, Co, and H₂O₂ according to Adams [22]. As a negative control, adjacent sections were subjected to reaction without TdT.

Southwestern histochemistry

The localization of estrogen-responsive element (ERE)-binding sites was examined by southwestern histochemistry, as described previously [23, 24]. Briefly, after deparaffinization, the sections were autoclaved at 120°C for 15 min in 0.01 M citrate buffer (pH 6.0). The sections were then reacted with a digoxigenin-labeled double-stranded DNA probe containing a complete palindromic ERE (vERE: 5'-GATCCAGGTCACAGTGACCTGGATC-3') of the chicken vitellogenin gene and a mutated ERE (mERE: 5'-GATCCAGATCACAGTGATCTGGATC-3') with two base mutations and a digoxigenin label at the 3'-end. To detect hybridized oligo-DNA probes, the sections were immunohistochemically stained with HRP-conjugated sheep anti-digoxigenin antibody by using a chromogen solution with DAB, Ni, Co, and H₂O₂.

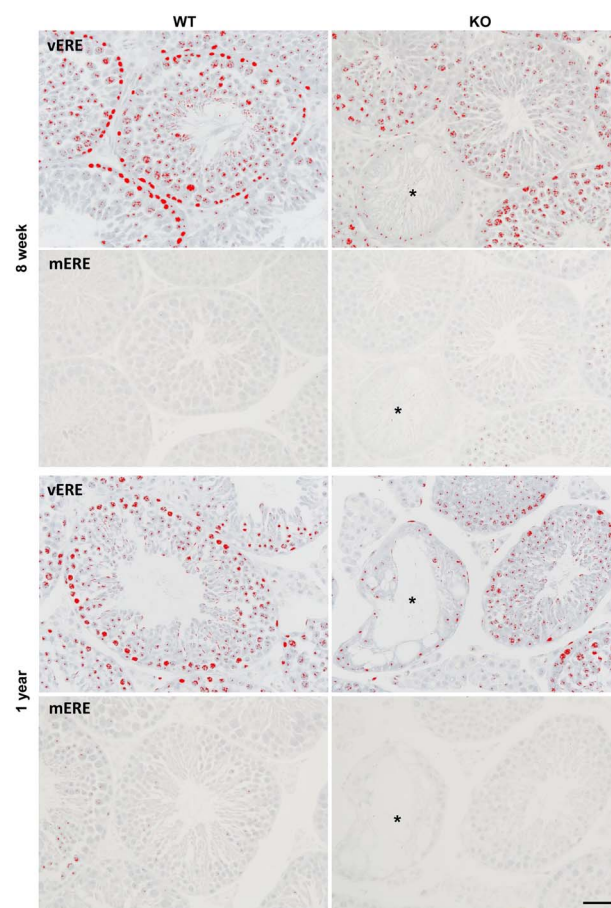


Figure 5. ERE-binding sites in HMGB2 KO mouse testis. vERE and mERE-binding sites were examined by southwestern histochemistry. Red color represents positive cells as determined by the image analyzer. All slides were analyzed under the same conditions, and positive cells were evaluated based on the staining density over the level of staining with the mERE probe. Asterisks indicate atrophic tubules. Scale bar: 50 μ m.

Quantitative analysis

Seminiferous tubules were counted in whole testicular cross-sections. In addition, Sox9-, PCNA-, and TUNEL-positive cells were counted in intact (ongoing spermatogenesis) and atrophic tubules were counted in whole cross-sections. In testicular cross-section, total area was measured by ImageJ. For image analysis of ERE, red color was assigned to the positive cells using Winroof software (Mitani, Tokyo, Japan). Positive cells were evaluated based on the staining density over the level of staining with the mERE probe.

Statistical analysis

All data are expressed as mean \pm SE. Statistical significance was assessed using the Student's *t*-test. The *P* < 0.05 was considered to be statistically significant. All analyses were performed with the Statistical Package for Social Sciences (version 20; IBM Corp., Armonk, NY, USA).

Results

HMGB2 KO induced seminiferous tubule atrophy

HMGB2 KO mice were born with the same body weight (BW) as their WT littermates, but their weight was $9.7 \pm 2.1\%$ lower when

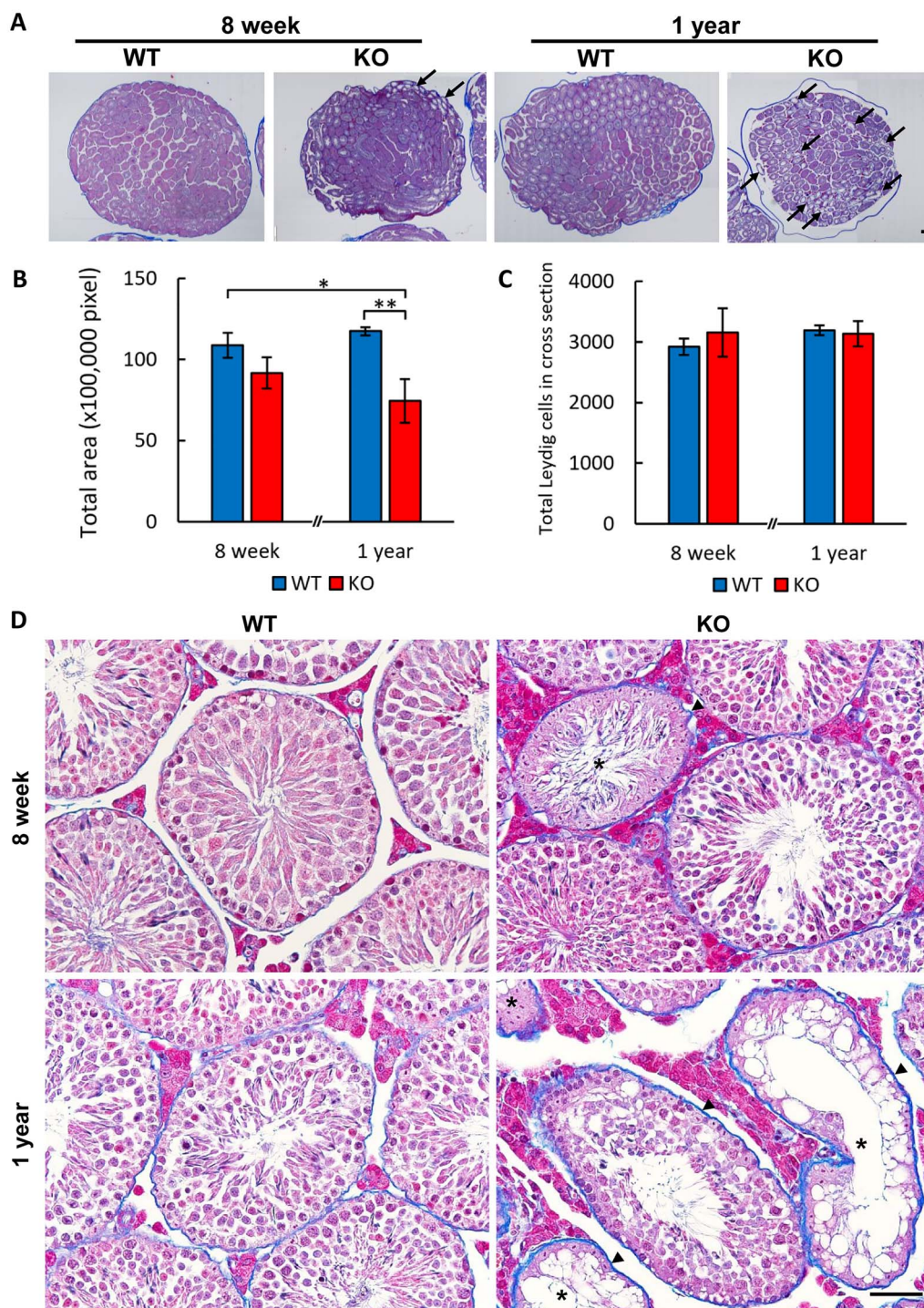


Figure 6. Increased Leydig cell density in HMGB2 KO mouse testis. Masson trichrome staining in cross-sections of WT and HMGB2 KO mouse testis (A). Seminiferous tubule atrophy is indicated by arrows. In the testis cross-section, total area was measured using ImageJ software, and the result is presented as a bar graph (B). Total number of Leydig cells in whole cross-sections (C). In the high-magnification microphoto, tubular membrane thickening is indicated by arrowheads (D). Asterisks indicate atrophic tubules. Scale bars: 200 μ m (A) and 50 μ m (D). Graphs represents mean \pm SEM. In each experimental group, three to five mice were used. * $P < 0.05$, ** $P < 0.01$. Student's t -test (two-tailed).

they reached 8 weeks of age. Compared with the decrease in BW, the testis weight was significantly decreased in KO mice at 8 weeks and 1 years of age (Figure 1A, Table 1). The efficiency of HMGB2 KO was examined by western blotting analysis (Figure 1B). In HE

staining, some of the seminiferous tubules in KO mouse testis were atrophic, as characterized by the absence of germ cells, tubule shrinkage, and diffuse collection of Leydig cells (Figure 1C). In WT mouse testis, expression of HMGB2 was found in spermatogonia to round

spermatids but was depleted in sperm (Figures 1C and 2A). The strongest HMGB2 expression was found in spermatocytes. HMGB2 protein was completely absent in KO mouse testis (Figure 1B and C). Interestingly, the number of seminiferous tubules was decreased in both 8-week-old and 1-year-old mice, but the number of abnormal tubules was significantly increased in the testis of aged KO mice (Figure 1D and E). All I–XII stages of seminiferous epithelial cycles were found in intact spermatogenic tubules, even in aged HMGB2 KO mouse testis (data not shown). Although the epididymis in HMGB2 KO mice was $18.3 \pm 6.5\%$ smaller than in WT littermates, there were no histopathological changes (data not shown). Moreover, mature sperm were found in the cauda epididymis of both WT and KO mice, indicating that germ cell development was not arrested at the specific developmental stage (data not shown). These results indicate that depletion of HMGB2 in KO mouse testis induces focal seminiferous tubule atrophy.

HMGB2 expression in germ cells

The HMGB2 expression in the testis was examined by immunofluorescence in WT and KO mice together with expression of Sox9, a marker of Sertoli cells (Figure 2A). In WT mouse testis, HMGB2 was expressed only in germ cells, but not in Sertoli cells. However, in KO mouse testis, all cells remaining in atrophic tubules were Sertoli cells. The number of Sox9-positive cells was significantly higher in atrophic tubules compared with intact tubules (Figure 2B).

Next, we examined the expression of HMGB2 together with the germ cell-specific marker DDX4/MVH (Figure 2C). In WT mouse testis, HMGB2 co-localized with DDX4/MVH in spermatocytes to round spermatids. In KO mouse testis, germ cells were absent in atrophic tubules. Collectively, these results indicate that atrophic tubules contain only Sertoli cells, but not germ cells. Moreover, the presence of tubules containing only Sertoli cells adjacent to intact spermatogenic tubules is characteristic of focal Sertoli cell only syndrome.

Decreased cell proliferation and increased apoptosis in HMGB2 KO mouse testis

Maintenance of the germinal epithelium depends upon the balance between germ cell proliferation, differentiation, and apoptosis. We examined cell proliferation by immunohistochemistry using PCNA in WT and KO mouse testis (Figure 3A). In WT mouse testis, proliferating cells were found in all seminiferous tubules. In HMGB2 KO mouse testis, proliferating cells were found in cycling tubules, but they were mostly absent in atrophic tubules. Cell proliferation was significantly decreased in 1-year-old HMGB2 KO mouse testis when compared with WT littermates (Figure 3B). In addition, Leydig cell proliferation was not significantly different in WT and HMGB2 KO mouse testis (data not shown). Apoptotic cells were examined by TUNEL staining, and the results are shown graphically in Figure 3C and D. The number of TUNEL-positive cells in the testis was comparable in 8-week-old WT and KO mice testis. In 1-year-old mice, the number of TUNEL-positive cells was significantly higher in the testis of KO mice. In summary, depletion of HMGB2 leads to decreased cell proliferation and increased apoptosis in the germinal epithelium.

Aberrant AR and ER α expression in HMGB2 KO mouse testis

Functional interactions between HMGB2 and steroid hormone receptors, such as the AR and ERs, have been reported [13, 14]. Therefore, we examined the expression of AR and ER α in WT

and KO mouse testis by using immunohistochemistry. In WT mouse testis, AR was expressed in Sertoli cells, myoepithelial cells, and Leydig cells (Figure 4A). In KO mouse testis, a normal distribution pattern in intact tubules was observed. However, in atrophic tubules, AR expression was decreased in Sertoli cells (arrows) but increased in Leydig cells. Next, we examined ER α expression in WT and KO mouse testis (Figure 4B). In WT mouse testis, Leydig cells and myoepithelial cells were positive for ER α . In KO mouse testis, the diffuse collection of Leydig cells led to an increase in the number of ER α -positive cells, especially in 1-year-old mouse testis. It is well known that ERs bind to EREs, which are specific consensus sequences in nuclear DNA, which function in the regulation of transcriptional activity of target genes. Therefore, we performed southwestern histochemistry to localize ERE-binding sites in tissue sections (Figure 5). In WT mouse testis, expression of vERE was observed mostly in spermatogonia, spermatocytes, and some spermatids. In HMGB2 KO mouse testis, vERE was markedly decreased in the seminiferous tubules. As a negative control, mERE was examined in all experiments, and it was not detected. These results indicate that sex steroid hormone receptors and ERE-binding sites were disrupted in HMGB2 KO mouse testis.

Increased Leydig cell density in HMGB2 KO mouse testis

In HMGB2 KO mouse, tubule atrophy with a peripheral localization was observed at 8 weeks of age, but this pattern was randomly distributed throughout the testis in aged mice (Figure 6A, arrows). The total area of the testis was measured in the testis cross-sections of WT and HMGB2 KO mouse by using Masson trichrome staining. Total area of the testis was significantly decreased in 1-year-old HMGB2 KO mouse when compared with WT littermates (Figure 6B). A diffuse collection of Leydig cells surrounding atrophic tubules was observed. The total number of Leydig cells in testicular cross-sections was determined, but no significant difference was observed (Figure 6C). These results indicate that the density of Leydig cells increased in HMGB2 KO mouse testis due to tubule shrinkage. Moreover, we examined thickening of the tubule membrane (Figure 6D). The seminiferous tubule membrane became thicker in HMGB2 KO mouse testis (arrowheads), and this increase in the hormonal barrier may have contributed to tubule atrophy.

HMGB1 expression was increased in HMGB2 KO mouse testis

The structural and functional similarities between HMGB2 and HMGB1 were reported previously [1]. Therefore, the co-localization of HMGB2 and HMGB1 was examined by immunofluorescence (Figure 7A). In WT mouse testis, HMGB1 was expressed in spermatogonia, Sertoli cells, myoepithelial cells, and Leydig cells. In the same tissue sections, HMGB2 co-localized in some spermatogonia (arrows). Increased expression of HMGB1 was observed in KO mouse testis, especially in 1-year-old mice. Furthermore, HMGB1 protein expression was confirmed by western blotting (Figure 7B), and densitometry analysis revealed a significant increase in HMGB1 expression in KO mouse testis (Figure 7C). Interestingly, in HMGB2 KO mouse testis, expression of HMGB1 was detected in spermatocytes (arrowheads) as well as spermatogonia. In order to confirm this finding, we performed double immunofluorescence staining for HMGB1 and synaptonemal complex protein 3 (SCP3), which is expressed in spermatocytes but not spermatogonia (Figure 8). In WT mouse testis, HMGB1 expression was limited to the spermatogonia, Sertoli cells, Leydig cells, and myoepithelial cells. Interestingly,

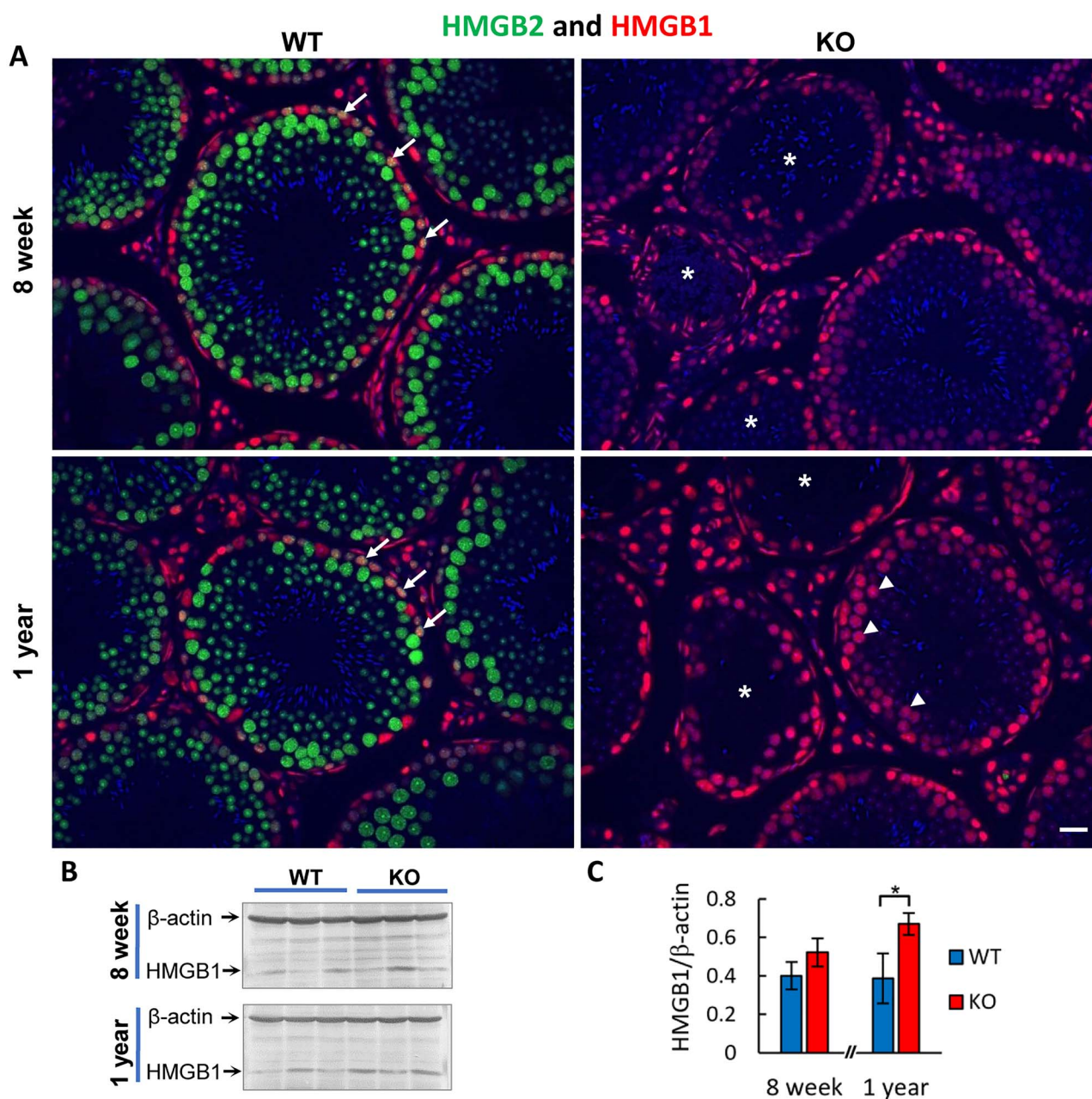


Figure 7. Expression of HMGB1 in WT and HMGB2 KO mouse testis. Double immunofluorescence for HMGB2 (green) and HMGB1 (red) in WT and HMGB2 KO mouse testis (A). Double positive cells were indicated by arrows. HMGB1-positive spermatocytes were indicated by arrowheads. Asterisks indicate atrophic tubules. Scale bar: 20 μ m. Western blotting analysis of HMGB1 in WT and KO mouse testis (B). Twenty micrograms of extracts from testis were subjected to 10% SDS-PAGE. HMGB1 (29 kDa) and β -actin (42 kDa) were detected in the same lane. Densitometry analysis of western blot (C). HMGB1 protein expression in each lane was normalized to that of β -actin. Data represent the mean \pm SE of three independent experiments. In each experimental group, three to five mice were used. * $P < 0.05$. Student's t -test (two-tailed).

co-localization of SCP3 and HMGB1 was observed in HMGB2 KO mouse testis, indicating that HMGB1 was also expressed in spermatocytes (arrows). Taken together, these results demonstrate that the loss of HMGB2 induced a compensatory increase in HMGB1 expression in spermatocytes.

Discussion

The main finding in this study is that depletion of HMGB2 induces aberrant expression of the AR and ER α , which leads to seminiferous tubule atrophy. Moreover, a compensatory increase in HMGB1

expression was observed in spermatocytes of HMGB2 KO mouse testis.

In WT mice, the abundant expression of HMGB2 in germ cells suggests HMGB2 plays a crucial role in spermatogenesis [9]. The selective expression of HMGB2 in germ cell lineage, but not in somatic cells, may be correlated with the high proliferative activity of male germ cells. A number of studies have demonstrated that cell proliferation is associated with HMGB2 expression during embryonic development, normal homeostasis, and malignancy [6, 7, 9]. Conversely, depletion of HMGB2 in senescent cells or aged tissues is

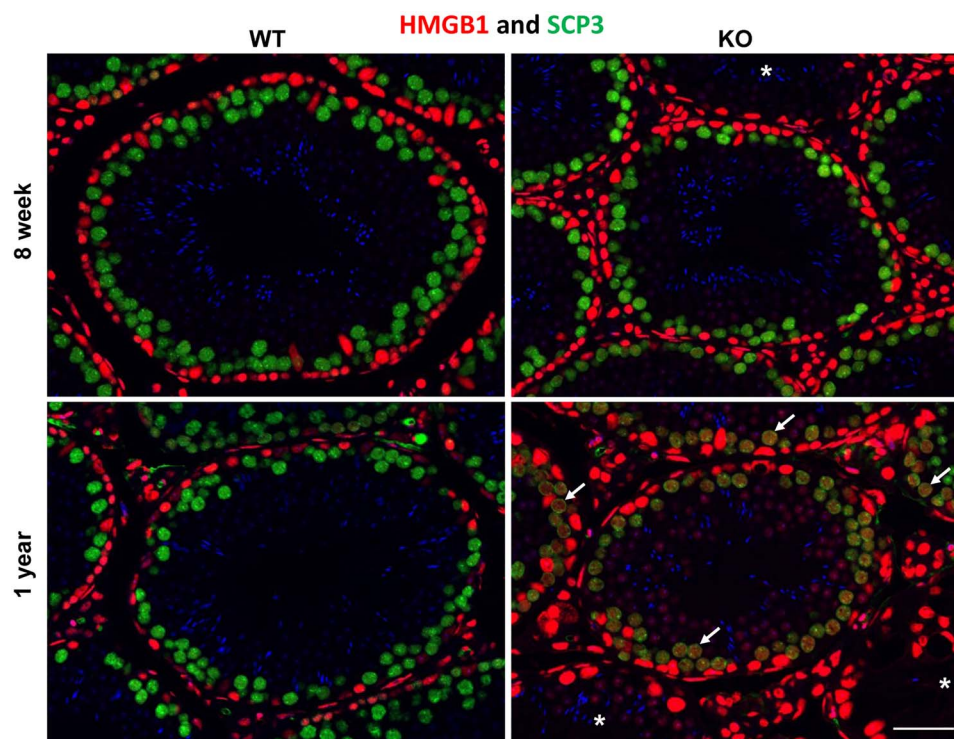


Figure 8. HMGB1 expression was increased in HMGB2 KO mouse testis. Double immunofluorescence for HMGB1 (red) and SCP3 (green) in WT and HMGB2 KO mouse testis. Arrows indicate HMGB1 expression in spermatocytes. Asterisks indicate atrophic tubules. Scale bar: 20 μ m.

associated with morphologic and functional abnormalities [4, 5]. In our study, we did not observe an aging-related decrease in HMGB2 expression in mouse testis at 1 years of age. This finding could be explained by the fact that 1-year-old mice are still fertile and that sterility starts at age over 2 years [25].

Depletion of HMGB2 led to atrophy of seminiferous tubules that contained Sertoli cells, but not germ cells. The adjacent tubules had an intact germinal epithelium, indicative of focal Sertoli cell only syndrome. A similar phenotype was observed in Foxa3-mutant mice, and this phenotype was characterized as focal Sertoli cell-only syndrome and sporadic tubular degeneration [26]. Few atrophic tubules were observed in the peripheral area in 8-week-old HMGB2 KO mouse testis, whereas atrophic tubules were significantly increased throughout the testis in 1-year-old HMGB2 KO mouse testis. These results indicate that the atrophy may start in one seminiferous tubule and subsequently progress. In our study, stages I–XII of the seminiferous epithelial cycle were observed in HMGB2 KO mouse testis. In addition, mature sperm were found in the cauda epididymis, indicating that germ cell development was not arrested at the specific developmental stage. In HMGB2 KO mouse testis, decreased germ cell proliferation and increased apoptosis led to progressive atrophy.

The causes of seminiferous tubule atrophy appear to be multifactorial, such as chemical toxicity, endogenous and exogenous androgens and estrogens, orchitis, irradiation, and ischemia [27]. In HMGB2 KO mice, disruption of sex steroid hormone signaling might have caused tubule atrophy via their receptors. It has been reported that HMGB2 functionally interacts with AR and ERs to enhance DNA binding and transcriptional activity via androgen-responsive elements and EREs [13, 14]. Moreover, genomic interactions between HMGB2 and ERs were identified in human breast cancer tissues [28]. As androgens and estrogens play critical roles in spermatogenesis, the increase in germ cell apoptosis resulting from

altered hormone transduction leads to seminiferous tubule atrophy [29]. In our study, the diffuse collection of Leydig cells surrounding atrophic tubules as well as aberrant expression of AR and ER α clearly indicate a disruption in paracrine signaling and hormonal transduction. Leydig cell hyperplasia was not found in HMGB2 KO mouse testis, indicating that the diffuse collection of Leydig cells appeared to be due to tubule shrinkage.

The functional relationship between HMGB1 and HMGB2 remains controversial. Some studies have reported that the differential expression of HMGB1 and HMGB2 indicates non-overlapping biological functions of these proteins at the cellular and tissue levels [1, 30]. On the other hand, strong evidence of complete interchangeability between HMGB1 and HMGB2 has also been reported [31]. During embryonic development, both HMGB1 and HMGB2 are expressed ubiquitously. After birth, HMGB1 continues to be expressed throughout the body. However, HMGB2 expression is limited to the testis and lymphatic tissues. The HMGB1 KO mice die after birth, but HMGB2 KO mice remain viable [1]. These results demonstrate that HMGB2 can function sufficiently in the absence of HMGB1 during embryonic development; however, it could not be rescued after HMGB2 expression decreases after birth. In WT mouse, HMGB1 was expressed in spermatogonia. However, HMGB1 expression was found in spermatogonia and spermatocytes in HMGB2 KO mouse testis. These findings clearly indicate a compensatory increase in HMGB1 expression in HMGB2 KO mouse testis. Notably, the strongest expression of HMGB2 was observed in spermatocytes in WT mouse testis. Therefore, in the absence of HMGB2, a compensatory increase in HMGB1 expression is observed in spermatocytes.

In summary, we demonstrated that depletion of HMGB2 induces aberrant expression of AR and ER α in the testis. Disrupted hormonal transduction leads to a decrease in germ cell proliferation and

increase in apoptosis, resulting in focal seminiferous tubule atrophy. Further studies will be required to elucidate the molecular mechanism of compensatory increase in HMGB1 expression in HMGB2-depleted mouse germ cells.

Acknowledgment

We would like to thank Momoe Yano and Ikuyo Tsuchimochi for technical assistance.

Conflict of interest

The authors have declared that no conflict of interest exists.

Data availability

Original micrographs and any other information are available upon request from the corresponding author.

References

- Bianchi ME, Agresti A. HMG proteins: dynamic players in gene regulation and differentiation. *Curr Opin Genet Dev* 2005; 15:496–506.
- Travers AA. Priming the nucleosome: a role for HMGB proteins? *EMBO Rep* 2003; 4:131–136.
- Ueda T, Yoshida M. HMGB proteins and transcriptional regulation. *Biochim Biophys Acta* 1799; 2010:114–118.
- Zirkel A, Nikolic M, Sofiadis K, Mallm JP, Brackley CA, Gothe H, Drechsel O, Becker C, Altmüller J, Josipovic N, Georgomanolis T, Brant L et al. HMGB2 loss upon senescence entry disrupts genomic organization and induces CTCF clustering across cell types. *Mol Cell* 2018; 70:730–744.
- Taniguchi N, Caramés B, Ronfani L, Ulmer U, Komiya S, Bianchi ME, Lotz M. Aging-related loss of the chromatin protein HMGB2 in articular cartilage is linked to reduced cellularity and osteoarthritis. *Proc Natl Acad Sci U S A* 2009; 106:1181–1186.
- Fu D, Li J, Wei J, Zhang Z, Luo Y, Tan H, Ren C. HMGB2 is associated with malignancy and regulates Warburg effect by targeting LDHB and FBP1 in breast cancer. *Cell Commun Signal* 2018; 16:8.
- Boström J, Sramkova Z, Salašová A, Johard H, Mahdessian D, Fedr R, Marks C, Medalová J, Souček K, Lundberg E, Linnarsson S, Bryja V et al. Comparative cell cycle transcriptomics reveals synchronization of developmental transcription factor networks in cancer cells. *PLoS One* 2017; 12:e0188772.
- Kimura A, Matsuda T, Sakai A, Murao N, Nakashima K. HMGB2 expression is associated with transition from a quiescent to an activated state of adult neural stem cells. *Dev Dyn* 2018; 247:229–238.
- Ronfani L, Ferraguti M, Croci L, Ovitt CE, Schöler HR, Consalez GG, Bianchi ME. Reduced fertility and spermatogenesis defects in mice lacking chromosomal protein Hmgb2. *Development* 2001; 128:1265–1273.
- Neto FT, Bach PV, Najari BB, Li PS, Goldstein M. Spermatogenesis in humans and its affecting factors. *Semin Cell Dev Biol* 2016; 59:10–26.
- O'Hara L, Smith LB. Androgen receptor roles in spermatogenesis and infertility. *Best Pract Res Clin Endocrinol Metab* 2015; 29:595–605.
- Carreau S, Bouraima-Lelong H, Delalande C. Estrogens in male germ cells. *Spermatogenesis* 2011; 1:90–94.
- Boonyaratnakornkit V, Melvin V, Prendergast P, Altmann M, Ronfani L, Bianchi ME, Taraseviciene L, Nordeen SK, Allegretto EA, Edwards DP. High-mobility group chromatin proteins 1 and 2 functionally interact with steroid hormone receptors to enhance their DNA binding in vitro and transcriptional activity in mammalian cells. *Mol Cell Biol* 1998; 18:4471–4487.
- Das D, Peterson RC, Scovell WM. High mobility group B proteins facilitate strong estrogen receptor binding to classical and half-site estrogen response elements and relax binding selectivity. *Mol Endocrinol* 2004; 18:2616–2632.
- Stros M. HMGB proteins: interactions with DNA and chromatin. *Biochim Biophys Acta* 1799; 2010:101–113.
- Srisowanna N, Chojjookhuu N, Yano K, Batmunkh B, Ikenoue M, Nhat Huynh Mai N, Yamaguchi Y, Hishikawa Y. The effect of estrogen on hepatic fat accumulation during early phase of liver regeneration after partial hepatectomy in rats. *Acta Histochem Cytochem* 2019; 52: 67–75.
- Chojjookhuu N, Sato Y, Nishino T, Endo D, Hishikawa Y, Koji T. Estrogen-dependent regulation of sodium/hydrogen exchanger-3 (NHE3) expression via estrogen receptor β in proximal colon of pregnant mice. *Histochem Cell Biol* 2012; 137:575–587.
- Buchwalow I, Samoilova V, Boecker W, Tiemann M. Multiple immunolabeling with antibodies from the same host species in combination with tyramide signal amplification. *Acta Histochem* 2018; 120:405–411.
- Chojjookhuu N, Hino S, Oo PS, Batmunkh B, Mohmand NA, Kyaw MT, Hishikawa Y. Ontogenetic changes in the expression of estrogen receptor β in mouse duodenal epithelium. *Clin Res Hepatol Gastroenterol* 2015; 39:499–507.
- Mai NNH, Yamaguchi Y, Chojjookhuu N, Matsumoto J, Nanashima A, Takagi H, Sato K, Tuan LQ, Hishikawa Y. Photodynamic therapy using a novel phosphorus Tetrphenylporphyrin induces an anticancer effect via Bax/Bcl-xL-related mitochondrial apoptosis in biliary cancer cells. *Acta Histochem Cytochem* 2020; 53:61–72.
- Hishikawa Y, Tamaru N, Ejima K, Hayashi T, Koji T. Expression of keratinocyte growth factor and its receptor in human breast cancer: its inhibitory role in the induction of apoptosis possibly through the overexpression of Bcl-2. *Arch Histol Cytol* 2004; 67:455–464.
- Adams JC. Heavy metal intensification of DAB-based HRP reaction product. *J Histochem Cytochem* 1981; 29:775.
- Batmunkh B, Chojjookhuu N, Srisowanna N, Byambatsogt U, Synn Oo P, Noor Ali M, Yamaguchi Y, Hishikawa Y. Estrogen accelerates cell proliferation through estrogen receptor α during rat liver regeneration after partial hepatectomy. *Acta Histochem Cytochem* 2017; 50: 39–48.
- Hishikawa Y, Damavandi E, Izumi S, Koji T. Molecular histochemical analysis of estrogen receptor alpha and beta expressions in the mouse ovary: in situ hybridization and southwestern histochemistry. *Med Electron Microsc* 2003; 36:67–73.
- Franks LM, Payne J. The influence of age on reproductive capacity in C57BL mice. *J Reprod Fertil* 1970; 21:563–565.
- Behr R, Sackett SD, Bochkis IM, Le PP, Kaestner KH. Impaired male fertility and atrophy of seminiferous tubules caused by haploinsufficiency for Foxa3. *Dev Biol* 2007; 306:636–645.
- Takano H, Abe K. Age-related histologic changes in the adult mouse testis. *Arch Histol Jpn* 1987; 50:533–544.
- Redmond AM, Byrne C, Bane FT, Brown GD, Tibbitts P, O'Brien K, Hill AD, Carroll JS, Young LS. Genomic interaction between ER and HMGB2 identifies DDX18 as a novel driver of endocrine resistance in breast cancer cells. *Oncogene* 2015; 34:3871–3880.
- O'Donnell L, Robertson KM, Jones ME, Simpson ER. Estrogen and spermatogenesis. *Endocr Rev* 2001; 22:289–318.
- Bagherpoor AJ, Kučirek M, Fedr R, Sani SA, Štros M. Nonhistone proteins HMGB1 and HMGB2 differentially modulate the response of human embryonic stem cells and the progenitor cells to the anticancer drug etoposide. *Biomolecules* 2020; 10:1450.
- Agresti A, Bianchi ME. HMGB proteins and gene expression. *Curr Opin Genet Dev* 2003; 13:170–178.